John M. Gomori, M.D.
Robert I. Grossman, M.D.
Herbert I. Goldberg, M.D.
Robert A. Zimmerman, M.D.
Larissa T. Bilaniuk, M.D.

Intracranial Hematomas: Imaging by High-Field MR[1]

Twenty intracranial hematomas between 1 day and over 1 year old were imaged using magnetic resonance at 1.5 T, with T1- and T2-weighted spin-echo pulse sequences. Characteristic intensity patterns were observed in the evolution of the hematomas, which could be staged as acute (<1 week old), subacute (>1 week and <1 month old), or chronic (>1 month old). Acute hematomas were characterized by central hypointensity on T2-weighted images (WIs). Subacute hematomas had peripheral hyperintensity on T1-WIs and then on T2-WIs. This hyperintensity proceeded to fill in the hematoma in the chronic stage. In subacute and chronic hematomas, there was hypointensity on T2-WIs in the immediately adjacent part of the brain. On T2-WIs of acute and subacute hematomas, the nearby white matter was characterized by hyperintensity, consistent with edema. A different mechanism is proposed for each of the three characteristic intensity patterns. Two of these mechanisms increase in proportion to the square of the magnetic field magnitude.

Index terms: Brain, hemorrhage, 13.367 • Brain, magnetic resonance studies, 13.1299

Radiology 1985; 157:87–93

Abbreviations Used:

ICH	intracerebral hematoma
PEDD	proton-electron dipole-dipole
PRE	proton relaxation enhancement
PT2	preferential T2
RBC	red blood cell
RE	reticuloendothelial
SDH	subdural hematoma
T1-WI	T1-weighted image
T2-WI	T2-weighted image

SIPPONEN et al. (1) recently reported their experience with the magnetic resonance (MR) imaging of intracerebral hematomas at 0.17 T. They noted some prolongation of the T1 relaxation time relative to white matter in acute (<7-day-old) hematomas. Their week-old hematomas displayed a peripheral ring of high intensity (shortened T1 and prolonged T2), which filled the entire hematoma cavity over subsequent weeks. This pattern has been noted previously (2–5). DeLaPaz et al. (6) found that the T1 and T2 of acute hematomas at 0.147 T were similar to those of white matter and that the high intensity of chronic hematomas was due to prolongation of T2. On partial saturation images (repetition time [TR], 150 msec) at 0.12 T, we found acute hematomas to be isointense to parenchyma, and chronic hematomas to be hyperintense (7).

In summary, at low magnetic fields (<0.5 T) acute hematomas are isointense to parenchyma while subacute and chronic hematomas are hyperintense on all pulse sequences. This study will describe the characteristic high-field MR findings in three stages (acute, subacute, and chronic) in the evolution of hematomas.

PATIENTS AND METHODS

Imaging was done using a 1.5-T superconducting MR imaging unit (General Electric, Milwaukee) using spin-echo (SE) pulse sequences (T1-weighted images [WIs]: TR, 600–800 msec; echo time [TE], 20–25 msec; T2-WIs: TR, 1,500–2,500 msec; TE, 40–120 msec). Seventeen patients were studied, and three patients had two separate hematomas each. There were 15 intracerebral hematomas (ICHs) aged 2 days to 16 months, four subdural hematomas (SDHs) aged 1 week to over 1 month, and one chronic epidural hematoma. All hematomas were diagnosed and staged by clinical and computed tomographic (CT) findings. Six ICHs and one SDH were confirmed surgically and pathologically.

RESULTS

Table 1 summarizes the stages of hematomas and the associated MR intensities. The acute (<7 days old) ICH was isointense or slightly hypointense to gray matter on T1-WIs and had a marked central hypointensity on T2-WIs (Fig. 1b and c). A peripheral ring of hyperintensity appeared within about a week on the T1-WI (Fig. 1d) and later on the T2-WI (Fig. 6b and c). The hyperintensity filled in the remainder of the hematoma cavity over the next week or two (Fig. 2). A similar sequence was observed with SDH (Fig. 3). The hyperintensity of hematomas may persist for over a year.

A parenchymal reaction adjacent to the hematoma appeared within a day or two and consisted of isointensity or mild hypointensity (like gray matter) on T1-WIs and hyperintensity on T2-WI (Figs. 1c and 2b). This slowly resolved over the subsequent weeks. After a week, the cerebral parenchyma immediately contiguous to the ICH developed a ring of marked hypointensity on the T2-WI, with isointensity or mild hypointensity on T1-WI (Figs. 2b and 4). This ring of parenchymal hypointensity persisted indefinitely and appeared only after the hematoma periphery was hyperintense on both T1- and T2-WIs. All the intensity patterns described can be

[1] From the Department of Radiology, Hospital of the University of Pennsylvania, Philadelphia. Received April 12, 1985; accepted and revision requested May 10, 1985; revision accepted May 21, 1985.

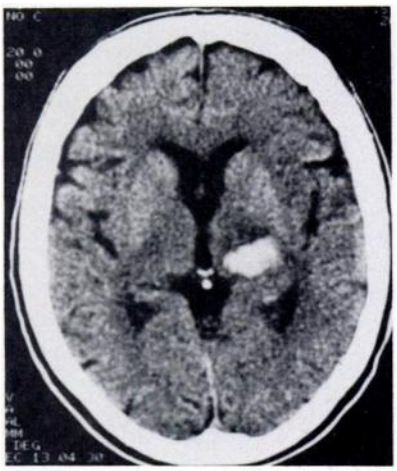

a.

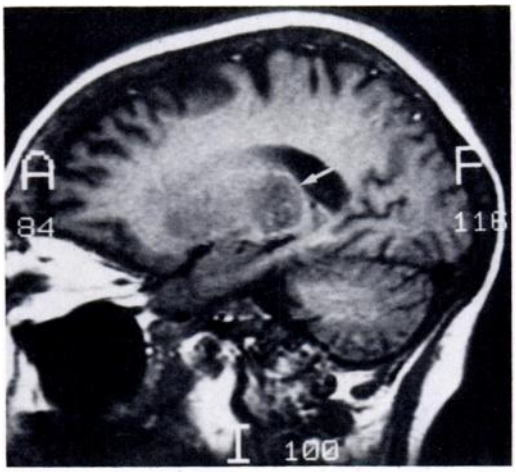

b.

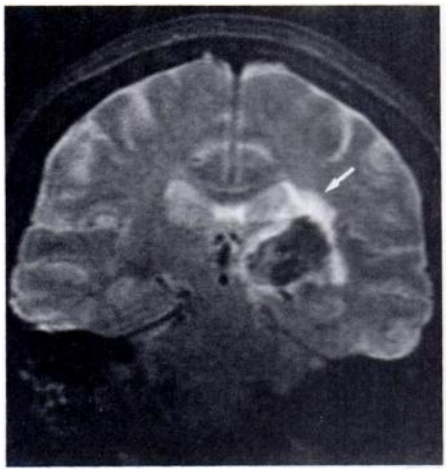

c.

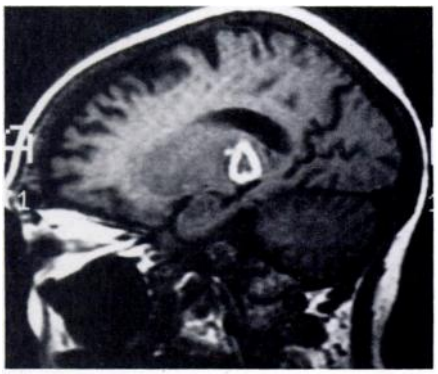

d.

Figure 1. Hypertensive left thalamic ICH in a 67-year-old woman. **(a)** Unenhanced CT scan within 12 hours of hemorrhage. **(b)** Sagittal T1-WI within 24 hours (TR, 600 msec; TE, 20 msec). The ICH (arrow) is isointense to gray matter. **(c)** Coronal T2-WI (TR, 2,000 msec; TE, 60 msec). The ICH is markedly hypointense to both the parenchyma and the converted cerebrospinal fluid. The perihematoma hyperintensity (arrow), not present on the T1-WI, is consistent with edema. **(d)** Sagittal T1-WI after 6 days (TR, 800 msec, TE, 20 msec). Peripheral hyperintensity has appeared.

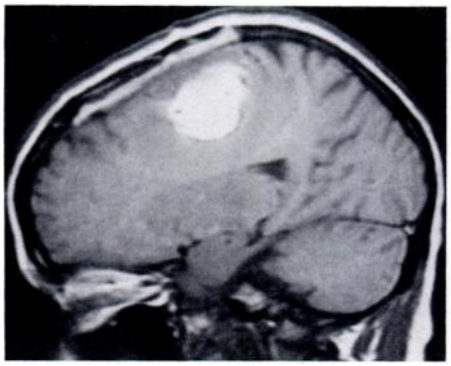

a.

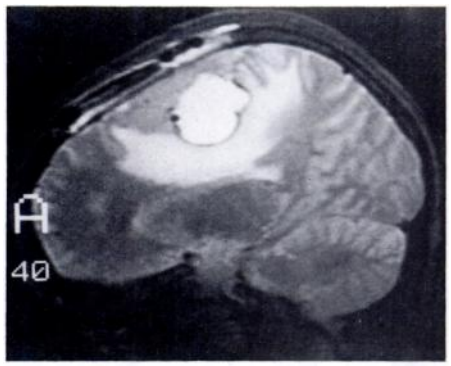

b.

Figure 2. ICH that developed immediately after partial resection of right parasagittal meningioma in a 37-year-old woman. **(a)** Sagittal T1-WI after 9 days (TR, 800 msec; TE, 20 msec). The ICH and a small SDH are hyperintense; separating them is the isointense residual meningioma. **(b)** Sagittal T2-WI (TR, 2,000 msec; TE, 70 msec). The ICH remains hyperintense, and the small SDH was not imaged in this section. There is a rim of hypointensity between the ICH and edematous brain below, but not between the ICH and the residual meningioma above. Hyperintensity of the white matter adjacent to the ICH is consistent with edema. Note that the ICH is more intense than the converted cerebrospinal fluid.

observed together (Fig. 4). The parenchymal T2-WI hypointensity adjacent to the hematoma was most prominent in normal brain tissue (Figs. 2b, 3c, and 5).

The CT hyperdensity of fresh hematomas corresponded to the central hypointensity on T2-WIs (Fig. 1). In a layering hematoma, the T2-WI hypointensity corresponded with the hyperdense dependent layer on the CT scan (Fig. 6). We obtained an intraoperative aspiration sample of a recent hematoma that had marked hypointensity on the T2-WI. Most of the red blood cells (RBCs) were intact, although some were crenated. There was no detectable methemoglobin. Pathologic study of the parenchymal rim of hypointensity on T2-WIs from three ICHs associated with tumors demonstrated hemosiderin-laden macrophages.

DISCUSSION

We have observed three characteristic intensity patterns in the evolution of hematomas: (*a*) the central hypointensity on the T2-WI in the acute stage, (*b*) the change to hyperintensity initially on the T1-WI and then on the T2-WI that extends from the hematoma periphery inward in the subacute stage, and (*c*) the rim of parenchymal hypointensity on the T2-WI in the brain abutting the hematoma in the subacute and chronic stages.

Two of these patterns (central hypointensity and parenchymal rim of hypointensity) occur only on MR images obtained at high magnetic fields. We would like to analyze these observations in light of our present knowledge of hematoma pathology and MR and propose possible mechanisms (Fig. 7, Table 2).

It is difficult to absorb extravasated blood from the brain parenchyma. A clot forms within a few hours after a hemorrhage, and its central portion contains intact and isolated RBCs. After approximately 3 weeks, the periphery of the hemorrhage changes from a reddish black to brown or orange, as macrophages digest the RBCs in the outer rim and produce hemosiderin. The remainder of the RBCs break down without being phagocytosed, producing either a chocolate-brown semiliquid material, containing mostly methemoglobin, or a firm, hard, red mass. After many months to years, a residual orange-walled slit is observed. Hemosiderin-laden macrophages in the walls of this cleft produce the orange stain and indicate old hemorrhage (8).

The CT scan of an acute ICH reveals hyperdensity ranging from that corresponding to whole blood (45% hematocrit) to that of clot (90% hematocrit) (9). The hyperdensity is secondary to the high protein concentration of the RBCs and is not related to the iron content (9). RBC lysis and

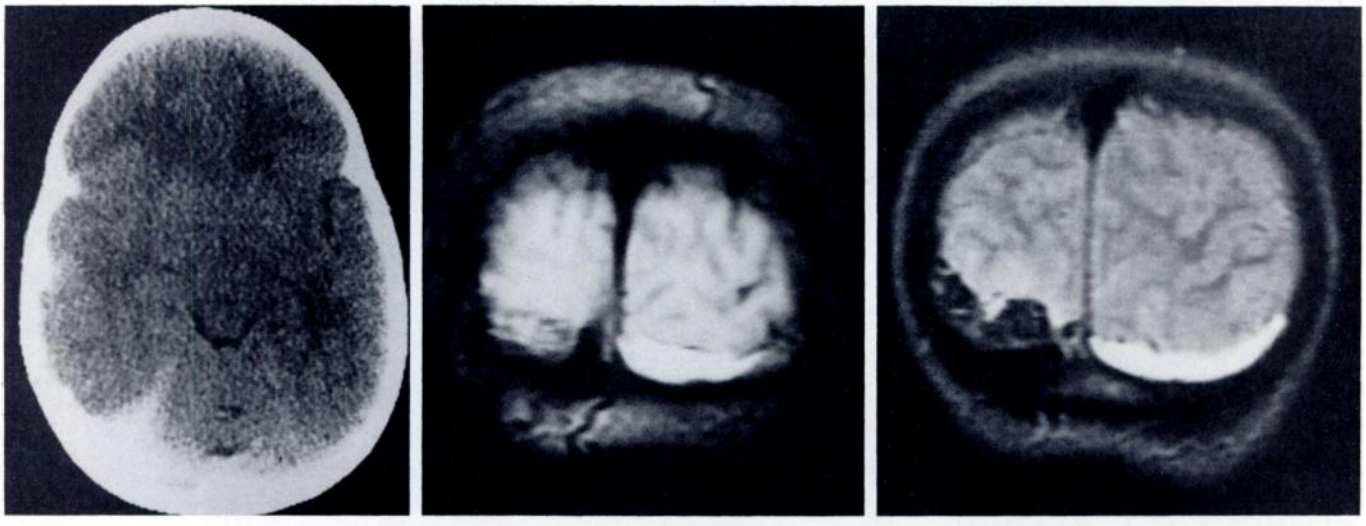

a. b. c.

Figure 3. **(a)** CT scan of 7-year-old hemophiliac with acute right subtemporal and suboccipital SDH (about 1 week old). **(b)** Coronal T1-WI (TR, 800 msec; TE, 20 msec). The recent right-sided suboccipital SDH is isointense to gray matter. An unsuspected chronic left-sided suboccipital SDH is homogeneously hyperintense. **(c)** Coronal T2-WI (TR, 2,000 msec; TE, 70 msec). The recent SDH is markedly hypointense, and the chronic SDH remains hyperintense. Note the lack of a hypointense rim around the chronic SDH.

Table 1
T1-WI/T2-WI Intensities Compared with Those of Parenchyma*

	Location			
Hematoma Stage	Hematoma Center	Hematoma Periphery	Rim of Brain Immediately Adjacent to Hematoma	White Matter Near Hematoma
Acute	=/≪	=/=	=/=	=/>
Subacute	=/<	</= proceeding to >/>	=/≪	=/>
Chronic	>/>	>/>	=/≪	=/=

Note.—First symbol indicates T1-WI intensity; second indicates intensity of T2-WI.
* > indicates increased intensity; <, decreased intensity; ≪, markedly decreased intensity; and =, no change in intensity.

Table 2
Relaxation Times*

	T1	T2
Intact RBCs with oxyhemoglobin	=	=
Intact RBCs with deoxyhemoglobin	=	≪
Intact RBCs with methemoglobin	≪	≪
Free methemoglobin	≪	>
Hemosiderin	=	≪
Edema	>	>

* > indicates prolongation of relaxation time; ≪, marked shortening of relaxation time; =, no change in relaxation time.

hemoglobin breakdown in the periphery of the hematoma are paralleled by progressive decrease in CT density and "size" (10). The hemosiderin rim surrounding the hematoma has been indirectly observed by the associated ring of enhancement, due initially to breakdown in the blood-brain barrier and subsequently to the formation of vascular granulation tissue (11). Rarely, the hemosiderin ring has been observed directly on unenhanced CT scans as an "iron rim" (12, 13).

The central hypointensity and parenchymal ring of hypointensity are most prominent on the T2-WIs. This implies a preferential T2 (PT2) proton relaxation enhancement (PRE) of water and has only been observed at high magnetic fields, indicating a dependence on magnetic field strength. For protons of liquid water, the only relaxation mechanism that will produce PT2 PRE dependent on magnetic field strength is that due to the dephasing of protons by the diffusion of water molecules through slowly varying, or static, local magnetic field gradients (14–16). This mechanism is proportional to the square of the local field gradients. Since there is no physiologic ferromagnetic material (17), biologic field gradients are due to heterogeneity in magnetic susceptibility and are directly proportional to the applied magnetic field; at 1.5 T, this will cause nine to 100 times the PT2 PRE effect of low fields (0.5–0.15 T). (The magnetic susceptibility of a substance is the proportionality constant between the applied magnetic field strength and the resultant local magnetization of the substance.) Normal biologic tissues do not exhibit field gradients large enough to cause significant PT2 PRE, even in field strengths above 1.5 T (18). A physiologically available paramagnetic relaxant with locally heterogeneous distribution that varies slowly, or not at all, must be present to produce a locally heterogeneous magnetic susceptibility. Local field gradients will then occur when a strong magnetic field is applied. A natural candidate, especially when hematomas are involved, would be some biologic form of iron.

Iron has four unpaired electrons in the ferrous (Fe^{+2}) state and five unpaired electrons in the ferric (Fe^{+3}) state (19). However, the Fe^{+2}-oxyhemoglobin complex has no unpaired electron spin. The Fe^{+2}-deoxyhemoglobin complex has four unpaired electrons and is paramagnetic (20). Fe^{+3} occurs in methemoglobin (21), ferritin, and hemosiderin (22). The most likely source of paramagnetic relaxation in the center of a fresh hematoma is Fe^{+2}-deoxyhemoglobin because methemoglobin, ferritin, and hemosiderin do not appear in the acute stage. For the familiar dipole-dipole PRE, the water proton must be able to come within 3 angstroms of the unpaired electron because this interaction is inversely proportional to the sixth power of the distance between the dipoles (19). Deoxyhemoglobin shows minimal proton-elec-

tron dipolar-dipolar (PEDD) PRE (23–25), apparently because of the inaccessibility to water protons of the unpaired electrons in Fe^{+2}-deoxyhemoglobin. However, Fe^{+2}-deoxyhemoglobin inside intact RBCs (clotted or unclotted), known to have a long correlation time (>10 seconds), will cause significant, slowly varying local heterogeneity of magnetic susceptibility, resulting in PT2 PRE at high magnetic fields (23). (The correlation time is the time it takes an entity to randomize its motion or orientation, i.e., to "forget" its previous condition [16].) Thulborn et al. (23) showed this phenomenon and demonstrated that this PT2 PRE was proportional to the square of the magnetic field, to the square of deoxyhemoglobin concentration, and to [hematocrit] × [100 − hematocrit]. The PT2 PRE varies from maximal to 36% of maximal as the hematocrit varies from 50% (whole blood) to 90% (clotted blood). Therefore, the PT2 PRE will probably be more sensitive to the deoxyhemoglobin concentration than to the hematocrit. When the RBCs were lysed, the magnetic field gradients disappeared, as did the PT2 PRE.

We propose that intact hypoxic RBCs with high deoxyhemoglobin concentrations are responsible for the central hypointensity of fresh hematomas in T2-WIs at high magnetic fields. Our one aspiration sample showed intact RBCs without methemoglobin.

Hemosiderin is the natural candidate for the paramagnetic relaxant causing the PT2 PRE in the part of the brain adjacent to the hematomas. Hemosiderin is more than 25% Fe^{+3}, it is water insoluble, and it is located mainly in the lysosomes of phagocytes (26). Its water insolubility precludes PEDD PRE due to the inaccessibility of the unpaired electrons to the water protons (19). Both lysosomes and macrophages have long correlation times, of the same order of magnitude as the correlation time of the RBCs (>10 seconds) (23). The heterogeneity of the hemosiderin distribution will produce heterogeneity of magnetic susceptibility and PT2 PRE proportional to the square of the main magnetic field strength. The brain's difficulty in removing blood degradation products is manifested by the persistence of the hemosiderin-laden macrophages (8) and explains the fact that the parenchymal T2-WI hypointensity is present mostly in the hematoma margins consisting of normally reacting brain. The thickness and magnitude of the hypointense rim should be indicative of the total amount of hemoglobin resorbed from old hematomas, that is, the number and extent of previous hemorrhages.

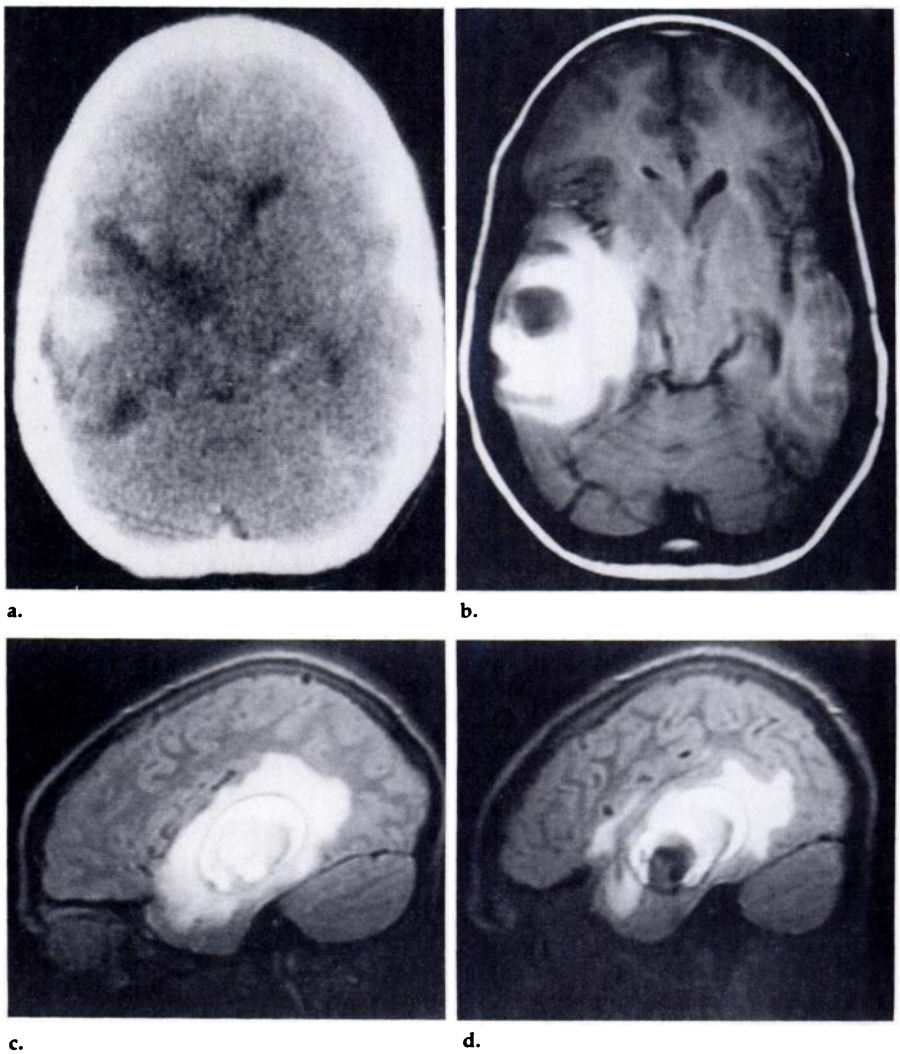

Figure 4. Small right temporal arteriovenous malformation and associated recent and aging ICHs in a 13-year-old boy. **(a)** Unenhanced CT scan within 2 days after occurrence of ICH. Recent hyperdense hematoma is surrounded by aging isodense hematoma. **(b)** Axial T1-WI (TR, 800 msec; TE, 20 msec). There is a large hyperintense region in the right temporal lobe with central hypointensity, slightly less intense than gray matter. These correspond to the isodense and hyperdense ICHs shown by CT. **(c)** Sagittal T2-WI through medial right temporal lobe (TR, 1,500 msec; TE, 40 msec). There is a moderately intense perihematoma edema and a ring of hypointensity surrounding a smaller ring of marked hyperintensity and an isointense center. **(d)** Sagittal T2-WI of the lateral portion of the right temporal lobe (TR, 1,500 msec; TE, 40 msec). Hypointense center of recent hematoma is surrounded by an edema-like intensity, probably due to some fluid collection.

In hemochromatosis, the reticuloendothelial (RE) cells of the liver, spleen, and bone marrow are loaded with hemosiderin. Brasch et al. (27) reported these to be hypointense on both T1- and T2-WIs at 0.35 T. They also observed hyperintensity of non-RE tissues on both T1- and T2-WIs. They proposed the PEDD PRE mechanism, which shortens T1 and T2 proportionally.

The SE intensity is proportional to $(e^{-TE/T2}) \times (1 - e^{TR/T1})$. When the TE is much less than the TR, the T1 shortening of the PEDD PRE of a dilute iron-compound (ferritin) solution would result in hyperintensity, as in the non-RE tissues, while a concentrated iron-compound solution (hemosiderin in the RE cells) would result in the hypointensity of the liver, spleen, and bone marrow present in hemochromatosis. If this is the correct PRE mechanism of tissue hemosiderin, then there should be no increase in PRE with magnetic field strength, no T2 relaxation preference, and we should observe hyperintensity in a second outer ring in ICHs, where the hemosiderin concentration falls off peripherally. None of these consequences was observed. In addition, PEDD PRE should not disappear at very low field strengths. However, hemochromatotic livers studied at 0.04 T showed only a mild decrease in T1 (130 ± 4 msec vs. 154 ± 11 msec in normal livers) (28). PEDD PRE does not explain the T2-WI hypointensity

Figure 5. Old hemorrhage in the cyst of a cerebellar astrocytoma in a 13-year-old boy. **(a)** Unenhanced CT scan. The astrocytoma is shown infiltrating the left cerebellar hemisphere, with a large midline cyst with anterior and left-sided calcifications. There are no calcifications in the right posterolateral cyst margin. **(b)** Sagittal T1-WI (TR, 800 msec; TE, 20 msec). The cyst is slightly hypointense to gray matter. **(c)** Axial T2-WI (TR, 2,000 msec; TE, 40 msec). The cyst fluid is hyperintense. Note the nondiscernibility of the calcium and the peripheral ring of hypointensity where the cyst abuts normal parenchyma rather than tumor.

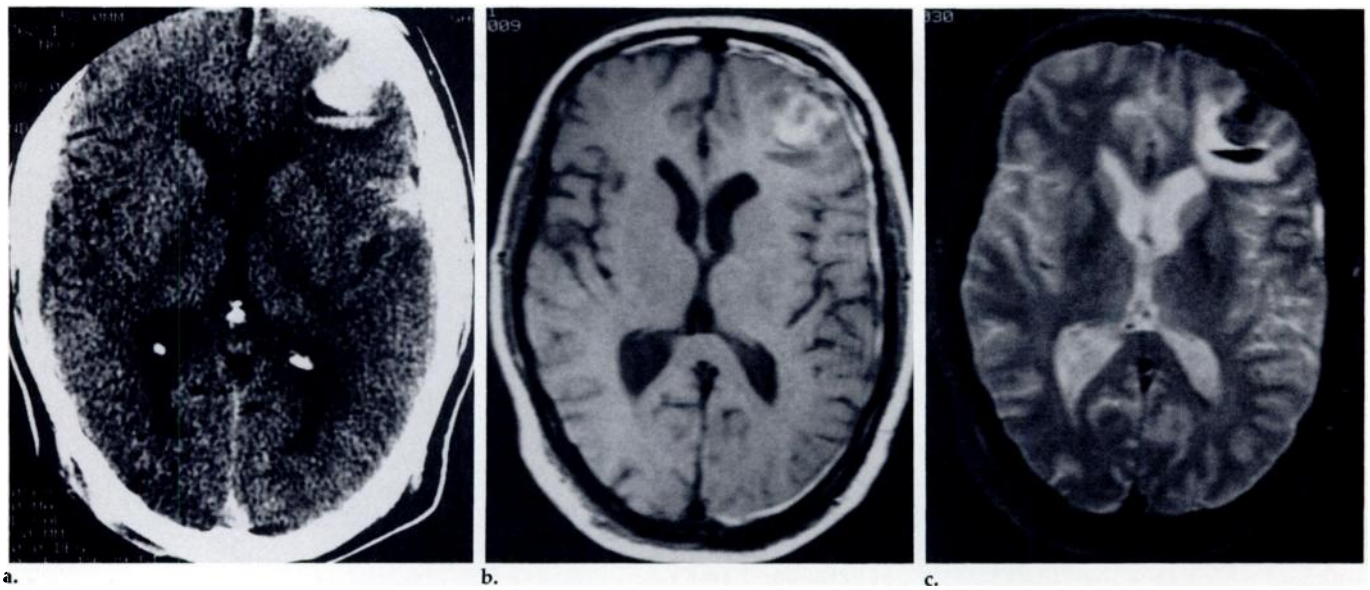

Figure 6. Head trauma in a 47-year-old man. **(a)** Unenhanced CT scan 2 days after trauma. The left-sided frontal ICH has two parts, one with a fluid-fluid level (layered separation of fluids of different densities). There is also a left temporal contusion. **(b)** Axial T1-WI 6 days after trauma (TR, 800 msec; TE, 25 msec). In the fluid-fluid level, the supernatant is isointense to white matter, and the dependent portion is slightly hypointense to gray matter. The other part of the ICH shows peripheral hyperintensity and a central isointensity to gray matter. There are small hyperintense SDHs in the left hemispheric and right frontal regions. **(c)** Axial T2-WI (TR, 2,500 msec; TE, 70 msec). Perihematoma edema is now appreciated as hyperintensity. The dependent hematoma and the center of the nonlayered hematoma are clearly hypointense. The region of hyperintensity on the T1-WI is isointense, and the supernatant is hyperintense.

of tissue hemosiderin and its variation with field strength. PT2 PRE due to heterogeneity in magnetic susceptibility is the likely mechanism for the hypointensity of hemosiderin on T2-WIs. The extremely high hemosiderin concentration in the RE cells in hemochromatosis may produce sufficient PT2 PRE, even at 0.35 T (but not at 0.04 T), so that the T2 is significantly shorter than the TE of 28 msec used by Brasch et al. in their T1-WIs. Therefore, the protons would have T2 relaxed (i.e., lost transverse magnetization) by the time of image acquisition and would appear hypointense. Wolf et al. (19) showed marked PT2 PRE of the livers of rabbits after intravenous injection of ferromagnetic iron particles, and they termed this effect "instant hemochromatosis." This PT2 PRE, due to field gradients of ferromagnetic heterogeneity, should not vary with field strength (15, 16).

What about the hyperintensity of non-RE tissues observed by Brasch et al. on both T1- and T2-WIs? Outside the RE cells, iron concentration is markedly decreased. Iron is present mostly in the form of intracellular ferritin, which is soluble and distributed relatively homogeneously in the cytoplasm (22, 26). Heterogeneity in

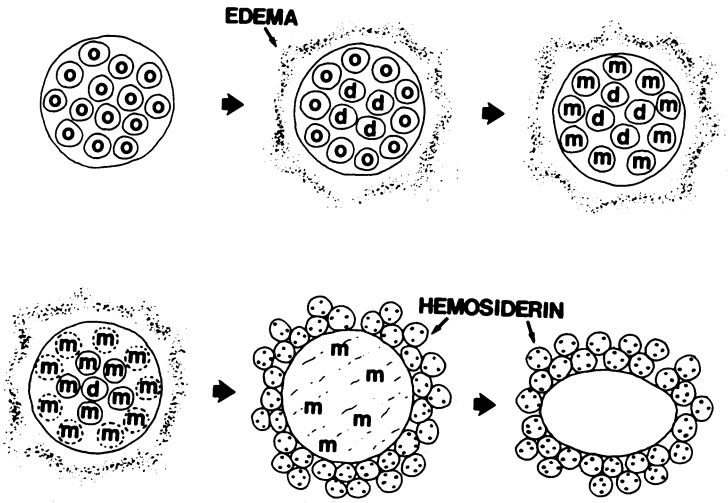

Figure 7. The stages of ICH evolution based on our observations in this study. *o* = oxyhemoglobin; *d* = deoxyhemoglobin; *m* = methemoglobin; circles = intact RBCs; dashed circles = RBC lysis; circles containing dots = macrophages laden with hemosiderin granules.

magnetic susceptibility is thus markedly reduced. The correlation time of ferritin is smaller than that of a cell by several orders of magnitude. If there is proton-electron access, then PEDD PRE will occur. This is unlikely because of the apparent inaccessibility of the iron in ferritin to iron stains (26). The hypothesis of Brasch et al. regarding PEDD PRE may apply to other soluble forms of iron. It would explain the hyperintensity of non-RE tissues in hemochromatosis on T1- and T2-WIs. Since ferritin is predominantly intracellular, a PT2 PRE effect (T2-WI hypointensity) should be noted at high fields because of heterogeneity in magnetic susceptibility.

The hyperintensity converging from the periphery to fill in the hematoma has also been observed at low magnetic fields (1–7). It appears to be caused by parallel T1 and T2 shortening and is similar to the PEDD PRE of dilute paramagnetic solutions (14, 16, 19). The delayed appearance and persistence of this hyperintensity correlate with the appearance of methemoglobin in aging hematomas (8). Fe^{+3}-methemoglobin has five unpaired electrons (21) that are accessible to water PEDD PRE, especially at low pH (29, 30). Neill et al. (31–33) demonstrated that in vitro autoxidation of hemoglobin to methemoglobin is greatly dependent on the oxygen tension. There were opposing effects of oxygen on the two chemical reactions involved. Methemoglobin is oxidized from deoxyhemoglobin, which is most abundant at zero oxygen tension. It is oxidized by the products formed during the oxidation of a number of substrates. However, these products are most abundant at high oxygen tensions. Thus, autoxidation of methemoglobin is negligible at zero or high oxygen tensions and is maximal at the relatively low tensions of about 20 mm Hg, when half the hemoglobin is in the deoxyhemoglobin form (21, 33).

The peripheral location of the hyperintensity seen on T1- and T2-WIs would correlate with the site of optimal concentration of deoxyhemoglobin and oxidizable substrates. RBC lysis should occur if the hyperintensity is to appear on the T2-WI. Otherwise, the exclusively intra-RBC presence of methemoglobin and deoxyhemoglobin will result in local heterogeneity in magnetic susceptibility and contribute significant PT2 PRE. The hyperintensity on the T1-WI precedes that on the T2-WI. This may indicate that RBC lysis lags behind methemoglobin production. Likewise, the parenchymal hemosiderin T2-WI hypointensity occurs only after the methemoglobin hyperintensity is also apparent on the T2-WI. This would be consistent with RBC lysis preceding hemoglobin degradation by the macrophages and the formation of hemosiderin. A decrease in hyperintensity of very old hematomas may result from resorption of the methemoglobin.

The hyperintensity surrounding recent hematomas on T2-WIs in the distribution of white matter has been observed at all field strengths (1, 6). It appears to be vasogenic edema and has been observed by CT (34).

The sensitivity to hemosiderin of T2-WIs in high-field MR suggests that nonhemorrhagic iron deposits may also be imaged as hypointense on T2-WIs due to PT2 PRE. Such deposits are present in the gray matter of the adult brain, especially in the gray matter of the extrapyramidal system. The pallidum and the red zone of the substantia nigra are most prominent (26). Our preliminary impression and recent observations of the extrapyramidal gray matter at 1.5 T (35) corroborate this. Iron deposits are also present in general paresis, cerebrotendinous cholesterolosis, and Hallervorden-Spatz syndrome (26).

CONCLUSION

We have observed characteristic PT2 PRE in the center of acute hematomas and in the adjacent parenchyma in subacute and chronic hematomas at magnetic field strengths of 1.5 T. Deoxyhemoglobin in intact RBCs is proposed as the cause of this finding in fresh hematomas. Hemosiderin in macrophage lysosomes of adjacent brain is the likely cause of the peripheral hypointensity pattern. These relaxation effects are proportional to the square of the magnitude of the main magnetic field. The peripheral hyperintensity extending inward in subacute hematomas on both T1-WI and T2-WIs has been noted at all field strengths. It is probably due to methemoglobin PEDD PRE. The perihematoma edema with hyperintensity on T2-WIs has also been observed at all field strengths and on CT scans. Figure 7 and Table 2 summarize our hypotheses for the evolution of ICH and the associated T1 and T2 changes. It seems, in short, that iron is to high-field MR what calcium is to CT. ■

Send correspondence and reprint requests to: Robert I. Grossman, M.D., Department of Radiology, Hospital of the University of Pennsylvania, 3400 Spruce St., Philadelphia, Pennsylvania 19104.

References

1. Sipponen JT, Sepponen RE, Sivula A. Nuclear magnetic resonance (NMR) imaging of intracerebral hemorrhage in the acute and resolving phases. J Comput Assist Tomogr 1983; 7:954–959.
2. Bailes DR, Young IR, Thomas DJ, Straughan K, Bydder GM, Steiner RE. NMR imaging of the brain using spin-echo sequences. Clin Radiol 1982; 33:395–414.
3. Bydder GM, Steiner RE, Young IR, et al. Clinical NMR imaging of the brain: 140 cases. AJR 1982; 139:215–236.
4. Brant-Zawadski M, Davis PL, Crooks LE, et al. NMR demonstration of cerebral abnormalities: comparison with CT. AJNR 1983; 140:847–854.
5. Pykett IL, Rosen BR, Buonanno FS, Brady TJ. Measurement of spin-lattice relaxation times in nuclear magnetic resonance imaging. Phys Med Biol 1983; 28:723–729.
6. DeLaPaz RL, New PFJ, Buonanno FS, et al. NMR imaging of intracranial hemorrhage.

J Comput Assist Tomogr 1984; 8:599–607.
7. Zimmerman RA, Bilaniuk LT, Grossman RI, et al. Resistive NMR of intracranial hematomas. Neuroradiology 1985; 27:16–20.
8. Adams RD, Sidman RL. Introduction to neuropathology. New York: McGraw-Hill, 1968; 177–178.
9. New PF, Aronow S. Attenuation measurements of whole blood and blood fractions in computed tomography. Radiology 1976; 121:635–640.
10. Dolinskas CA, Bilaniuk LT, Zimmerman RA, Kuhl DE. Computed tomography of intracerebral hematomas. I. Transmission CT observations on hematoma resolution. AJR 1977; 129:681–688.
11. Laster DW, Moody DM, Ball MR. Resolving intracerebral hematoma: alteration of the "ring sign" with steroids. AJR 1978; 130:935–939.
12. Som PM, Patel S, Nakagawa H, Anderson PJ. The iron rim sign. J Comput Assist Tomogr 1979; 3:109–112.
13. Russel EJ: Complete ring on noncontrast CT could indicate aging hemorrhage. AJNR 1984; 4:997–998.
14. Bloembergen N, Purcell EM, Pound RV. Relaxation effects in nuclear magnetic resonance absorption. Physiol Rev 1948; 73:679–712.
15. Robertson B. Spin-echo decay of spins diffusing in a bounded region. Physiol Rev 1966; 151:273–277.
16. Slichter CP. Principles of magnetic resonance. Berlin: Springer-Verlag, 1980; 174–183.
17. Brittenham GM, Farrell DE, Harris JW, et al. Magnetic susceptibility measurements of human iron stores. N Engl J Med 1982; 307:1671–1675.
18. Packer KJ. The effects of diffusion through locally inhomogeneous magnetic fields on transverse nuclear spin relaxation in heterogeneous systems: proton transverse relaxation in striated muscle tissue. J Magn Reson 1973; 9:438–443.
19. Wolf GL, Burnett KR, Goldstein EJ, Joseph PM. Contrast agents for magnetic resonance imaging. In: Kressel HY, ed. Magnetic resonance annual 1985. New York: Raven, 1985; 231–266.
20. Pauling L, Coryell C. The magnetic properties and structure of hemoglobin, oxyhemoglobin, and carboxyhemoglobin. Proc Natl Acad Sci USA 1936; 22:210–216.
21. Bodansky O. Methemoglobinemia and methemoglobin-producing compounds. Pharmacol Rev 1951; 3:144–196.
22. Fairbanks VF, Beutler E. Iron metabolism. In: Williams WJ, Beutler E, Erslev AJ, Rundles RW, eds. Hematology. New York: McGraw-Hill, 1977; 168–177.
23. Thulborn KR, Waterton JC, Matthews PM, Radda GK. Oxygenation dependence of the transverse relaxation time of water protons in whole blood at high field. Biochim Biophys Acta 1982; 714:265–270.
24. Fabry TL, Reich HA. The role of water in deoxygenated hemoglobin solutions. Biochem Biophys Res Commun 1966; 22:700–703.
25. Singer JR, Crooks LE. Some magnetic studies of normal and leukemic blood. J Clin Eng 1978; 3:237–243.
26. Lindenberg R. Tissue reactions in the gray matter of the central nervous system. In: Haymaker W, Adams RD, eds. Histology and histopathology of the nervous system. Vol. 1. Springfield: Thomas, 1982; 1130–1142.
27. Brasch RC, Wesbey GE, Gooding CA, Koerper MA. Magnetic resonance imaging of transfusional hemosiderosis complicating thalassemia major. Radiology 1984; 150:767–771.
28. Runge VM, Clanton JA, Smith FW, et al. Nuclear magnetic resonance of iron and copper disease states. AJR 1983; 141:943–948.
29. Eisenstadt M. NMR relaxation of protein and water protons in methemoglobin solutions. Biophys J 1981; 33:469–474.
30. Koening SH, Brown RE, Lindstrom TR. Solvent and the heme region of methemoglobin and fluoro-methemoglobin. Biophys J 1981; 34:397–408.
31. Neill JM. Studies on the oxidation-reduction of hemoglobin and methemoglobin. III. The formation of methemoglobin during the oxidation of autoxidizable substance. J Exp Med 1925; 41:551–560.
32. Neill JM. Studies on the oxidation reduction of hemoglobin and methemoglobin. IV. The inhibition of "spontaneous" methemoglobin formation. J Exp Med 1925; 41:561–570.
33. Neill JM, Hasting AB. The influence of the tension of molecular oxygen upon certain oxidations of hemoglobin. J Biol Chem 1925; 63:479–492.
34. Goldberg HI. Stroke. In: Lee SH, Rao KCVG, eds. Cranial computed tomography. New York: McGraw-Hill, 1983; 642.
35. Drayer BP, Burger P, Riederer S, et al. High-resolution magnetic resonance for mapping brain iron deposition. Presented at the 23d Annual Meeting of the American Society of Neuroradiology, New Orleans, February 18–23, 1985.